Oncogenic BRAF ^{V600E} induces glial proliferation through ERK and neuronal death through JNK

Qing Ye
Shanghai University of TCM: Shanghai University of Traditional Chinese Medicine
Nasser Al-Kuwari
Harvard Medical School
Pranay Srivastava
Harvard Medical School
Xiqun Chen (xchen17@mgh.harvard.edu)
Harvard Medical School https://orcid.org/0000-0001-8582-8891

Research

Keywords: BRAF, mutation, neurons, microglia, astrocytes, inflammation, cell death, cell proliferation

Posted Date: February 23rd, 2021

DOI: https://doi.org/10.21203/rs.3.rs-220057/v1

Abstract

Background

Activating V600E in BRAF is a common driver mutation in cancers of multiple tissue origins, including melanoma and glioma. $BRAF^{V600E}$ has also been implicated in neurodegeneration. The present study aims to characterize $BRAF^{V600E}$ on cell death and survival in three major cell types of the CNS: neurons, astrocytes, and microglia.

Methods

Multiple primary cultures and cell lines of glial cells and neurons were employed. $BRAF^{V600E}$ as well as $BRAF^{WT}$ expression was mediated by lentivirus or retrovirus. Blockage of downstream effectors were achieved by siRNA. Gene expression data from patients with Parkinson's disease was analyzed.

Results

In astrocytes and microglia, $BRAF^{V600E}$ induces cell proliferation, and the proliferative effect in microglia is mediated by activated ERK but not JNK. Conditioned medium from $BRAF^{V600E}$-expressing microglia induced neuronal cell death. In neuronal cells, $BRAF^{V600E}$ directly induces cell death, through JNK but not ERK. We further show that BRAF-related genes are enriched in pathways in patients with Parkinson's disease.

Conclusions

Our study identifies distinct consequences mediated by distinct downstream effectors in dividing glial cells and in neurons following the same BRAF mutational activation and a causal link between BRAF-activated microglia and neuronal cell death that does not require physical proximity. It provides insight into a possibly important role of BRAF in neurodegeneration as a result of either dysregulated BRAF in neurons or its impact on glial cells.

Background

The BRAF (v-Raf murine sarcoma viral oncogene homolog B) gene encodes a serine-threonine kinase. BRAF is ubiquitously expressed, with high levels in neuronal tissues [1]. As part of the Ras–Raf–MEK–ERK pathway, BRAF is activated by RAS at the upstream, and it in turn phosphorylates and activates mitogen activated protein kinase (MEK) kinase at the downstream. MEK then phosphorylates and activates extracellular signal-regulated kinase (ERK). The Ras–Raf–MEK–ERK signaling cascade transduces extracellular signals to the cytoplasm and nucleus and is involved in the regulation of cell

survival, growth, proliferation, and differentiation in developing and adult tissues, such as the central nervous system (CNS). In non-neuronal cells, including glial cells, BRAF stimulates cell proliferation [2]. BRAF signaling is both necessary and sufficient to promote astrocyte proliferation during development [3]. Mutations of BRAF, predominantly valine-to-glutamic acid mutation at residue 600 (V600E) lead to constitutive kinase activation and unregulated cell growth and proliferation. $BRAF^{V600E}$ is one of the most prevalent oncogenic mutations in human cancers, accounting for more than half melanomas and many other cancers including a variety of pediatric and adult gliomas [4]. Accordingly, BRAF inhibitors have been developed as a therapy for cancer [5].

The essential role of BRAF in neuronal development and survival has also been supported by a number of studies [6,7]. BRAF is essential for survival of embryonic neurons in culture [1]. Homozygous BRAF null mice are embryonic lethal due to growth retardation and neuronal defects [8]. Mice expressing non-functional BRAF in neural stem cell-derived brain tissue displayed disturbed neuronal circuits in the cerebellum and hippocampus, along with impaired neuronal generation [9]. Forebrain-specific knockout of BRAF caused impaired hippocampal learning and memory [10]. Further, BRAF controls synaptic transmission and learning behavior [11]. Mutant $BRAF^{V600E}$ in neural progenitors resulted in a hyperexitable phenotype in neocortical pyramidal neurons [12], and it contributes to intrinsic epileptogenicity without the formation of any neuronal tumors, whereas high proliferation of glial lineage cells contributes to the tumorigenity of the mutation [13]. Constitutive activation of BRAF by low-level expression of $BRAF^{V600E}$ in the mouse germline is associated with increased number of astrocytes with unaltered neuron number in hippocampal area [14].

More recent evidence implicates that BRAF activity may be involved in neuronal cell death, directly or indirectly. $BRAF^{V600E}$ somatic mutation in the erythro-myeloid progenitors, which give rise to tissue-resident myeloid cells caused clonal expansion of microglia and subsequently caused synaptic loss and neuronal death in adulthood [15]. The degenerative changes can be prevented by BRAF inhibition [16].

Here we report distinct consequences and downstream effectors following $BRAF^{V600E}$ expression in primary cultures and cell lines of three major cell types of the CNS: neurons, astrocytes, and microglia. We also show indirect effects of $BRAF^{V600E}$ on neurons through astrocytes and microglial cells.

Methods

Constructs and viral vectors

Constructs used were: pMD2.G (Addgene, Cat# 12259, USA), psPAX2 (Addgene, Cat# 12260, USA), pHAGE-$BRAF^{V600E}$ plasmid (Addgene, Cat# 116204, USA), pHAGE-$BRAF^{WT}$ plasmid (Addgene, Cat# 116719, USA), pBabe-Puro-$BRAF^{V600E}$ plasmid (Addgene, Cat# 15269, USA) , gag/pol-Retroviral plasmid (Addgene, Cat# 14887, USA), Control siRNA (Cell Signaling Technology, Cat# 6568S, USA), SAPK/JNK siRNA (Cell Signaling Technology, Cat# 6232S, USA), ERK1 siRNA (Cell Signaling Technology, Cat# 6436S, USA), ERK2 siRNA (Cell Signaling Technology, Cat# 6578S, USA).

Lentiviral particles were produced by transducing HEK293T cells with MD2.G envelope plasmid (Addgene), psPAX2-LV package plasmid (Addgene) and Lipofectamine 2000 Transduction Reagent (Thermo Fisher Scientific, USA).

Retroviral particles were produced by transducing HEK293T cells with the pBabe-Puro-BRAF-V600E plasmid (Addgene), the packaging plasmid gag/pol-Retroviral (Addgene), and the envelope plasmid MD2.G using Lipofectamine 2000.

Microglial cell line BV2 cells

BV2 cells (ATCC, Cat# CRL-2467, USA) were cultured with high-glucose DMEM (Gibco) containing 10% FBS (Gibco) and high glucose DMEM/F-12 (Gibco) containing 10% FBS at 37°C in 5% CO2 under constant temperature and humidity. After transduction with $BRAF^{V600E}$, $BRAF^{WT}$, and vector lentivirus, respectively, for 24 h, cells were cultured for 24 h in DMEM/F12 without FBS, and then medium and cells were collected for subsequent experiments.

Human neuroblastoma cell line SH-SY5Y cells

SH-SY5Y cells (ATCC, Cat# CRL-2266, USA) were seeded at 80% density, the medium was changed to DMEM/F12 supplemented with 1% FBS and 10 mM retinoic acid (Sigma, USA) for differentiation for 3 days [17]. The medium was then replaced with conditioned medium from BV2 cells transduced with different vectors for 24 h. Cells were then collected at different time points for subsequent experiments.

Primary cortical mixed culture

Primary cortical mixed culture was prepared from C57BL/6J mice embryonic day 17. To obtain cortical culture, pregnant mice (the Jackson Laboratory) were anesthetized, embryos were dissected, and cortex was collected in PBS on ice. Tissue was incubated in 0.25% trypsin–EDTA (Gibco) at 37°C for 15 min. Trypsinized tissue was transferred into high-glucose DMEM/F12 medium supplemented with 10% FBS. After centrifugation (1000×g, 5 min), the pellet was resuspended [17,18]. Cells were plated onto poly(L-lysine)-coated 24-well plates at 10^6 cells per well and cultured in NB-A (Gibco). Cortical mixed cells were cultured for 5 days, then transduced with lentivirus (LV) vectors or retrovirus (RV) vectors for 24 h, and then cultured in NB-A medium for 96 h.

Primary cortical neuronal culture

Primary cortical neurons were prepared from C57BL/6J mice embryonic day 17. The dissected cortical tissue was digested, triturated and centrifuged as for cortical mixed culture. Cells were plated onto poly (L-lysine)-coated 24-well plates at 10^6 cells per well and cultured in NB-A with 2% B27 (Invitrogen, USA). After 24 h in culture, 5ug/ml cytarabine was added to inhibit the growth of glial cells in the medium, and then changed to the original medium 48 h later. Neurons were cultured for 5 days, and then transduced with $BRAF^{V600E}$, or $BRAF^{WT}$, or vector lentivirus plus 8 μg/ml polybrene (Sigma–Aldrich, USA) for 24 h. After transduction, cells were cultured in NB-A for 120 h and then collected for subsequent experiments.

Primary microglial culture

Mixed glial cells were obtained from C57BL/6 mice embryonic day 17. Cells were cultured in high-glucose DMEM/F12 supplemented with 10% FBS in humidified air containing 5% CO2 at 37°C. The culture medium was replaced with fresh medium 24 h after the initial preparation and every 3 days thereafter. After 1 week, microglial cells were obtained by mechanical shaking of the mixed glial cell cultures for 1 h. Cells were routinely monitored for purity by ionized calcium binding adaptor molecule 1 (Iba1) staining and the population of Iba1+ cells was >95% [19,20]. Microglial cells were seeded at 80% density, then transduced with $BRAF^{V600E}$, or $BRAF^{WT}$, or vector lentivirus plus 8 μg/ml polybrene for 24 h. After transduction, the cells were cultured for 120 h in high-glucose DMEM/F12 with or without FBS, and the medium as well as the cells were collected for subsequent experiments.

Primary astrocyte culture

Primary astrocytes were obtained from C57BL/6 mice embryonic day 17. The dissected cortical tissue was digested, triturated and centrifuged as for neuronal cultures. The cell pellet was resuspended in high-glucose DMEM/F12 supplemented with 10% FBS. Cells were seeded in poly-L-ornithine-coated Petri plates. Nonadherent cells were removed after 20 min [21]. Astrocytes were transduced with $BRAF^{V600E}$, or $BRAF^{WT}$, or vector lentivirus plus 8 μg/ml polybrene for 24 h. After transduction, the cells were cultured for 120 h in high-glucose DMEM/F12 with or without FBS, and the medium as well as the cells were collected for subsequent experiments. All experiments were performed in accordance with a protocol approved by Institutional Animal Care and Use Committee at Massachusetts General Hospital.

siRNA transfection

Primary neurons and microglial cells were seeded in 6-well plates and transfected with ERK1 siRNA (Cell Signaling Technology, USA), ERK2 siRNA (Cell Signaling Technology), SAPK/JNK siRNA (Cell Signaling Technology) at 80% cell confluence on day 4 in culture. ERK1 siRNA, ERK2 siRNA, JNK siRNA and Lipofectamine RNAiMAX Transfection Reagent (Thermo Fisher Scientific) were diluted in OPTI-MEM medium (Thermo Fisher Scientific), mixed gently, and incubated for 5 min to allow complex formation. The cells were transfected by adding the RNAi–Lipofectamine complex dropwise to medium to achieve a siRNA concentration of 100 nmol/l. The cells were collected 48 h after the transfection for subsequent experiments [22].

Cell cycle determination

Cells were seeded in 6-well plates at 70% confluence, followed by virus transduction and siRNA treatment for 3 days. The cells were collected, fixed in 70% ethanol overnight, and stained with Tali Cell Cycle Kit (Thermo Fisher Scientific). We used the Attune NxT Flow Cytometer (Thermo Fisher Scientific) to determine the percentage of cells in each cell cycle phase. Flowjo software was used to analyze the data.

NO and LDH and MTS assays

Griess Reagent Kit (Thermo Fisher Scientific) was used to assess NO according to the manufacturer's instructions. Cells were seeded in 96-well plates. We mixed the following reagents in each well: 20 µl Griess Reagent, 150 µl nitrite-containing sample, and 130 µl deionized water. A photometric reference was prepared by mixing 20 µl Griess Reagent and 280 µl deionized water. Absorbance of the nitrite-containing samples relative to the reference was measured in Synergy 2 Multi-Mode Microplate Reader (Bio-Tek, USA) at 548 nm.

For LDH assay, Pierce LDH Cytotoxicity Assay Kit (Thermo Fisher Scientific) was used. 50 µl cell culture medium was transferred to a new 96-well plate, 50 µl reaction mixture was added to each well and incubated at room temperature for 30 min, then 50 µl stop solution was added. Absorbance at 490 and 680 nm was measured using Synergy 2 Multi-Mode Microplate Reader (Bio-Tek , USA).

For MTS assay, MTS Cell Proliferation Colorimetric Assay Kit (BioVision, USA) was used. Cells were seeded in 96-well plates and treated as indicated above. After the treatment, cell culture medium of each well was removed and 110 µl reagent containing 10 µl MTS and 100 µl medium was added to each well and incubated in humidified air containing 5% CO2 at 37°C for 1 h. Absorbance at 490 nm was measured using a microplate reader.

Immunostaining and quantitative analysis

Cells were seeded in 24-well plates. After treatment, the medium was removed and the plates were washed with PBS three times, the slides were fixed with 4% paraformaldehyde for 15 min and washed with PBS three times, and permeabilized with 0.5% Triton X-100 at room temperature for 20 min. Plates were washed with PBS. 5% goat serum was added and incubated at room temperature for 30 min. Primary antibodies were added and incubated at 4°C overnight. Primary antibodies used were microtubule-associated protein 2 (MAP2) (1:500, Thermo Fisher Scientific), Iba1 (1:500, Abcam, USA), Ki-67 (1:100, Thermo Fisher Scientific), and glial fibrillary acidic protein (GFAP) (1:1000, Sigma–Aldrich,) Plates were washed with PBS and incubated with secondary antibody: goat anti-rabbit IgG-Alexa Fluor 488 (1:500, Molecular Probes, USA) or donkey anti-mouse IgG-Alexa Fluor 546 (1:500, Thermo Fisher Scientific) for 45 min in the dark at room temperature, washed with PBS, and stained with DAPI (Vector Laboratories, USA). For analysis of fluorescence intensity, images were captured under an Olympus BX51 microscope (Olympus Optical Co., Tokyo, Japan) with Olympus CAST stereology software and a DP 70 digital camera system using the same camera gain, exposure time and pixel setting for all samples. Integrated optical density (IOD) of staining in the images was analyzed by Image J.

RNA extraction and real-time quantitative PCR analysis

RNA was isolated using the TRIzol LS Reagent (Thermo Fisher Scientific). SuperScript III First-Strand Synthesis System (Thermo Fisher Scientific) was used for cDNA synthesis. All primers were obtained from Massachusetts General Hospital DNA Core and are listed in Table 1. StepOnePlus Real-Time PCR System (Thermo Fisher Scientific) was used. Relative gene expression levels were analyzed using the 2-ΔΔCt method. GAPDH was used as internal control.

Western blotting

Western blotting was applied to detect BRAF, ERK, JNK, nuclear factor kappa-B (NF-κB), and other proteins associated with the pathways. Primary antibodies included BRAF (1:100, Thermo Fisher Scientific), MEK1/2 antibody (1:1000, Cell Signaling Technology), phospho-MEK1/2 antibody (1:1000, Cell Signaling Technology), ERK1/2 (1:1000, Cell Signaling Technology), phospho-ERK1/2 (1:1000, Cell Signaling Technology), JNK (1:1000, Cell Signaling Technology), phospho-JNK (1:1000, Cell Signaling Technology), NF-κB p65 (1:1000, Cell Signaling Technology), phospho-NF-κB p65 (1:1000, Cell Signaling Technology). GAPDH (1:5000, Proteintech, China) was used as internal control. RIPA lysis buffer containing PMSF Protease Inhibitor (Thermo Fisher Scientific) and Pierce Phosphatase Inhibitor (Thermo Fisher Scientific) were used to extract cell total protein. Protein concentration was determined by Pierce BCA Protein Assay Kit (Thermo Fisher Scientific). Equal amounts of protein (30 mg) were loaded onto SDS-PAGE. Following separation, proteins were transferred from the gels to methanol-activated polyvinylidene fluoride (PVDF; Sigma–Aldrich) transfer membranes, blocked with 5% BSA for 1 h at 37°C. The membranes were incubated with primary antibodies overnight at 4°C. Subsequently, the membranes were incubated with an appropriate horseradish-peroxidase-labeled secondary antibody for 1 h at room temperature. Proteins were visualized using an ECL system (Thermo Fisher Scientific). The expression levels of phosphorylated proteins were quantified by normalizing to their respective total proteins. Data was analyzed using ImageJ software.

ELISA

The release of Interleukin 1β (IL-1β), Interleukin 6 (IL-6) and tumor necrosis factor α (TNF-α) in mouse primary microglial cell culture medium was measured with commercial ELISA kits-Mouse IL-1β (R&D Systems, USA), mouse IL-6 (R&D Systems), and mouse TNF-α (R&D Systems). Cells were seeded in 6-well plates and cultured with DMEM/F12 supplemented with 10% FBS. After virus transduction, the cells were cultured for 24 h in DMEM/F12 without FBS, and the medium was collected, centrifuged at 3000 rpm for 10 min, and the supernatant was subjected to ELISA. Absorbance at 450 nm was measured using Synergy 2 Multi-Mode Microplate Reader (Bio-Tek). IL-1β, IL-6 and TNF-α concentrations were calculated based on the standards and normalized with total protein concentration of the same sample.

Statistical analysis

All experiments were repeated at least three times with at least three replicates within each condition. Investigators who performed assays were blind to treatment groups. All values are presented as the mean ± SEM. Group comparisons were performed using ANOVA and Tukey's post hoc test. $P < 0.05$ was considered statistically significant. Postmortem SN (substantia nigra) gene expression profile from patients with Parkinson's disease and function enrichment analysis of BRAF-related genes GDS2821 gene expression data from 16 Parkinson's disease patients was obtained from the National Center for Biotechnology Information's (NCBI) Gene Expression Omnibus (GEO: https://www.ncbi.nlm.nih.gov/geo). Raw data were normalized and processed by R software (version 3.3.3) with the limma package [23] and the normalized gene expression levels were presented as log2-transformed values. The Spearman coefficients of expression of genes and BRAF were calculated, whilst the expression genes with $P < 0.05$ were defined as BRAF-related genes. The Database for Annotation, Visualization, and Integrated Discovery (DAVID, http://david.ncifcrf.gov), an online functional annotation tool were applied for gene ontology (GO) enrichment analyses including biological process (BP), cellular component (CC) and molecular function (MF), and Kyoto Encyclopedia of Genes and Genomes (KEGG) pathway analysis [24]. GO terms or KEGG pathways with $P < 0.01$ were considered statistically significant.

Results

BRAF ^{V600E} expression leads to neuronal cell death and glial cell proliferation in primary mouse cortical mixed culture

Primary cortical mixed culture composing of neurons and glial cells (astrocytes and microglia was transduced with LV expressing human $BRAF^{V600E}$, or human $BRAF^{WT}$, or control vector. BRAF overexpression was detected by Western blotting, which showed significantly increased BRAF in transduced cells than vector or non-transduced control cells (Fig. 1A). Immunostaining for MAP2, a marker of neurons and Iba1, a marker for microglia 120 h after the transduction showed that there was a decrease in the number of neurons and an increase in the number of microglia in the mixed culture transduced with $BRAF^{V600E}$ than vector or $BRAF^{WT}$ (Fig. 1A). Similarly, immunostaining for MAP2 and GFAP, a marker for astrocytes showed that there was a decrease in the number of neurons and an increase in the number of astrocytes in the culture transduced with $BRAF^{V600E}$ than vector or $BRAF^{WT}$. $BRAF^{WT}$ did not change the number of either MAP2 + or iba1 + or GFAP + cells (Fig. 1C). These results suggest $BRAF^{V600E}$ expression in the cortical mixed culture may lead to different outcomes for neurons and glial.

We next transduced the mixed cultures with $BRAF^{V600E}$ or control vector by RV. Unlike LV, which is capable of infecting both neurons and glial cells, RV infects only dividing cells, not postmitotic neurons. After 120 h, MAP2 and Iba1 staining showed an increase in the number of microglia and a decrease in the number of neurons in RV $BRAF^{V600E}$-transduced culture than RV vector-transduced culture (Fig. 1B). $BRAF^{V600E}$ transduction resulted in an increase in the number of astrocytes and a decrease in the number of neurons than RV vector-transduced cells, which were demonstrated by MAP2 and GFAP staining (Fig. 1D). These

findings suggest that the mutant BRAF may cause neuron loss through proliferation of microglia and/or astrocytes.

$BRAF^{V600E}$ expression in astrocytes promotes proliferation

To investigate $BRAF^{V600E}$ effect on individual cell types, we next transduced primary astrocytes prepared from C57BL/6 mouse embryos with lentiviral $BRAF^{V600E}$, $BRAF^{WT}$ and control vector, respectively. Western blotting showed that, 120 h after the transduction, expression levels of mitogen-activated protein (MAP)/phosphorylated MEK1/2 (p-MEK1/2), phosphorylated ERK1/2 (p-ERK1/2) in $BRAF^{V600E}$-transduced astrocytes were increased compared with the vector-transduced or non-transduced control groups, suggesting activation of the ERK pathway by $BRAF^{V600E}$ (Fig. 2A). Flow cytometry showed that there was a lower percentage of cells in G0/G1 phase and a higher percentage of cells in S phase in $BRAF^{V600E}$-transduced astrocytes as compared with vector or non-transduced control groups (Fig. 2B). Despite an increase in BRAF expression by nearly 3-fold, $BRAF^{WT}$ did not change cell cycle distribution in cultured primary astrocytes, which can be explained by approximately 500-fold greater kinase activity of $BRAF^{V600E}$ than $BRAF^{WT}$ [25]. MTS assay revealed that astrocyte viability was increased significantly 96 and 120 h after $BRAF^{V600E}$ transduction compared with vector or non-transduced control group (Fig. 2C). Immunostaining for GFAP and Ki67, an indicator of proliferation, showed that total number of GFAP + cells and percentage of Ki67 + cells in $BRAF^{V600E}$-transduced group were significantly higher than vector or non-transduced control group 96h after transduction, while transduction with $BRAF^{WT}$ showed no significant difference compared with vector or the control group (Fig. 2D). IL-6, IL-10, and cyclooxygenase 2 (COX2) were increased at mRNA level whereas TNF-α and IL-1β were decreased after $BRAF^{V600E}$ transduction. In addition, nuclear factor erythroid 2 (NF-E2)-related factor 2 (Nrf2) and its downstream genes heme oxygenase 1 (HO1), quinone oxidoreductase 1 (NQO1), glutamate cysteine ligase catalytic subunit (GCLC), and glutamate cysteine ligase modifier subunit (GCLM) were increased significantly in $BRAF^{V600E}$-transduced astrocytes. In addition, there was a dramatic increase in glial-derived neurotrophic factor (GDNF) mRNA level in $BRAF^{V600E}$-transduced cells (Fig. 2E).

$BRAF^{V600E}$ expression in microglia induces cell proliferation and activation through ERK

To determine $BRAF^{V600E}$ effects on microglial cells, we transduced BRAF into BV2 cells for 96 h. Western blotting showed that expression of BRAF, p-MEK1/2, p-ERK1/2, and phosphorylated nuclear factor kappa-B (NF-κB) p65 (p-NF-κB p65) in the $BRAF^{V600E}$ group was dramatically increased compared with vector and non-transduced control groups (Figure S1A). Flow cytometry showed lower percentages of cells in G0/G1 and G2/M phases and higher percentage of cells in S phase in $BRAF^{V600E}$-transduced group compared with vector or non-transduced control groups (Figure S1B). MTS also revealed that transduction with $BRAF^{V600E}$ induced BV2 cell proliferation (Figure S1D). Immunostaining for Iba1 showed that cell number in $BRAF^{V600E}$-transduced group was significantly increased compared with

vector and non-transduced control groups. Morphologically, BV2 cells showed a typical branching shape at the resting state in non-transduced control group. Transduction with vector and $BRAF^{WT}$ caused no obvious morphological changes compared with the control group. BV2 cells transduced with $BRAF^{V600E}$ displayed reduced cell area, loss of ramifications, and development of an amoeboid shape (Figure S1C). qPCR analysis showed increases in TNF-α, IL-1β, IL-6, and COX2 in $BRAF^{V600E}$-treated BV2 cells. mRNA levels of Nrf2 and its downstream genes HO1, NQO1, GCLC, and GCLM were decreased significantly after transduction with $BRAF^{V600E}$ compared with vector and non-transduced control groups (Figure S1F). ELISA showed that inflammatory factors (IL-1β, IL-6, TNF-α) secreted into the culture medium by $BRAF^{V600E}$-treated BV2 cells was higher than in the control groups (Figure S1G). There was no significant difference in NO levels among the groups (Figure S1E). These results support proliferation and activation of BV2 microglia by $BRAF^{V600E}$.

We next employed mouse primary microglia to further characterize $BRAF^{V600E}$ effects in microglial cells. Cells were transduced with BRAF vectors for 120 h. $BRAF^{V600E}$ transduction significantly increased p-MEK1/2 and p-ERK1/2. In addition, p-NF-κB p65 as well as p- JNK were increased (Fig. 3A). To determine the roles of activated ERK and JNK in $BRAF^{V600E}$ effects, we transduced microglial cells with siRNA targeting JNK (si-JNK), siRNA targeting ERK (si-ERK), and control-siRNA. Knockdown efficiency of si-JNK and si-ERK was demonstrated by Western blotting (Fig. 3B). After treatment with si-ERK, $BRAF^{V600E}$-transduced microglia showed significantly downregulated ERK as compared with control-siRNA treated cells expressing $BRAF^{V600E}$. NF-κB phosphorylation was similarly downregulated. si-JNK did not change p-NF-κB in $BRAF^{V600E}$-transduced microglia (Fig. 3C). Iba1 staining showed that the cell number and percentage of Ki67 + cells in $BRAF^{V600E}$-treated group were significantly increased compared with vector and non-transduced control groups. $BRAF^{WT}$-treated group did not show significant difference from vector and non-transduced control groups (Fig. 3D). si-ERK treatment blocked $BRAF^{V600E}$-induced proliferation of microglia. si-JNK did not change Iba1 + cell number and percentage of Ki67 + cells in $BRAF^{V600E}$-transduced cells (Fig. 3E). Non-transduced control microglia displayed the typical branching shape at the resting state. Transduction with vector, $BRAF^{WT}$ and $BRAF^{V600E}$ plus si-ERK caused no obvious morphological changes compared with the control group. $BRAF^{V600E}$ and $BRAF^{V600E}$ plus si-JNK transduction induced enlargement of the microglial cell body, loss of ramifications, and development of an amoeboid shape (Fig. 3D and 3E).

Flow cytometry showed that, compared with vector group, percentage of S phase microglia in $BRAF^{V600E}$-treated group was increased, and this effect of $BRAF^{V600E}$ was diminished when cells are treated with si-ERK but not si-JNK (Fig. 3F). MTS assay revealed higher cell viability after transduction with $BRAF^{V600E}$ for 96 and 120 h compared with vector and non-transduced control groups, and si-ERK reversed this effect (Fig. 3G). Inflammatory markers TNF-α, IL-1α, IL-1β, IL-6, human inducible NO synthase (iNOS), and COX2 were increased at the mRNA level after transduction with $BRAF^{V600E}$ for 120 h. $BRAF^{WT}$-transduced microglia displayed similar trends but to a lesser extent, supporting BRAF activity dependence of the changes. si-ERK significantly inhibited $BRAF^{V600E}$-induced inflammatory gene expression, while si-JNK

did not reverse the effect (Fig. 3I). ELISA and nitrite release showed that inflammatory factors (IL-1β, IL-6, TNF-α) and NO secreted by microglia after treatment with $BRAF^{V600E}$ were higher than vector and non-transduced control groups. si-ERK, but not si-JNK reversed secretion of inflammatory factors (IL-1β, IL-6, TNF-α) and NO induced by $BRAF^{V600E}$ (Fig. 3H and Fig. 3J).

Conditioned medium from $BRAF^{V600E}$-expressing microglial cells but not astrocytes induces neuronal cell death

We treated differentiated SH-SY5Y cells with conditioned medium from BV2 cells transduced with $BRAF^{V600E}$, $BRAF^{WT}$, vector, or from non-transduced control cells for 24 h. MAP2 staining showed a significantly loss of neuronal cells in differentiated SH-SY5Y cells cultured with BV2-$BRAF^{V600E}$ conditioned medium as compared to cells cultured with BV2-vector and BV2-$BRAF^{WT}$ conditioned medium. Consistently, these cells showed increased lactate dehydrogenase (LDH) release. Differentiated SH-SY5Y cells cultured with BV2-control, BV2-vector and BV2-$BRAF^{WT}$ conditioned medium exhibited no obvious changes in cell numbers and LDH release as compared to the control group (Figure S2).

We next treated primary cortical neurons with conditioned medium from astrocytes transduced with $BRAF^{V600E}$, $BRAF^{WT}$, vector, or from non-transduced control cells for up to 72 h. Astrocytes transduced with $BRAF^{V600E}$ were proliferating with upregulated GDNF, certain cytokines and antioxidants as shown in Fig. 2. However, no significant difference in number of MAP2 + was demonstrated in all astrocyte conditioned medium-treated groups compared with the control group. LDH release showed no significant change among groups at 24, 28, and 72 h (Fig. 4A).

Primary cortical neurons were in parallel treated with conditioned medium from primary microglia transduced with $BRAF^{V600E}$, $BRAF^{WT}$, vector, or from non-transduced control cells for 72 h. A significant decrease in the number of MAP2 + cells were demonstrated in cells treated with microglia-$BRAF^{V600E}$ conditioned medium (Fig. 4B). $BRAF^{V600E}$ conditioned medium also induced LDH release in primary neurons (Fig. 4C). Treatment with microglia-control, microglia-vector and microglia-$BRAF^{WT}$ conditioned medium did not result in changes compared to the control group. Similar neurotoxicity was demonstrated in microglia-$BRAF^{V600E}$ + si-JNK conditioned medium group, but not in microglia-$BRAF^{V600E}$ + si-ERK conditioned medium group, suggesting that the indirect, toxic effects of $BRAF^{V600E}$ on neurons resulted from ERK-mediated changes in microglia (Fig. 4A and 4B).

$BRAF^{V600E}$ expression in neurons directly promotes cell death through the JNK pathway

To characterize direct neuronal effects of $BRAF^{V600E}$, primary cortical neurons were transduced with $BRAF^{V600E}$ $BRAF^{WT}$, and vector for 24 h. The cells were then cultured for 96 h in neural culture basal medium. Western blotting confirmed BRAF overexpression and higher levels of p-MEK1/2, p-ERK1/2, p-JNK, caspase-3 and c-Jun in the $BRAF^{V600E}$-treated group as compared with vector and non-transduced

control groups (Fig. 5A). Marked increases in c-Jun, B cell leukemia/lymphoma-2 (Bcl-2), Bcl-2 associated X protein (Bax), p53, Fas-ligand (FasL), and TNF-α at the mRNA level were observed after transduction with $BRAF^{V600E}$ for 120 h (Fig. 5B). $BRAF^{V600E}$ induced significant neurotoxicity as demonstrated by loss of MAP2 + cells and release of LDH in $BRAF^{V600E}$-transduced neurons compared with vector- and non-transduced neurons (Fig. 5C).

si-JNK and si-ERK were used to block signals downstream to BRAF. Knockdown efficiency of si-JNK and si-ERK was verified by Western blotting (Figure S3). Reduced p-JNK, caspase-3, and c-Jun was demonstrated in neurons treated with si-JNK + $BRAF^{V600E}$ as compared with cells treated with $BRAF^{V600E}$ (Fig. 5D). At mRNA level, si-JNK reversed $BRAF^{V600E}$-induced changes in c-Jun, Bax, Bcl-2, p53, Fasl and TNF-α in cultured cortical neurons (Fig. 5E). Treatment with si-ERK blocked p-ERK and total ERK expression induced by $BRAF^{V600E}$ (Fig. 5G). There was no significant difference in protein expression of p-JNK, caspase-3 and c-Jun or mRNA expression of c-Jun, Bax, Bcl-2, p53, Fasl and TNF-α between $BRAF^{V600E}$ and $BRAF^{V600E}$ + si-JNK groups (Fig. 5G and 5H). These results suggest that activation of the JNK pathway by $BRAF^{V600E}$ is independent of $BRAF^{V600E}$-induced ERK activation. MAP2 staining as well as LDH assay showed significantly reduced number of MAP2 + cells and higher LDH release in cells transduced with $BRAF^{V600E}$ and the changes were partially reversed after co-treatment with si-JNK (Fig. 5F). si-JNK also inhibited JNK in vector-transduced neurons but without significant influences on c-Jun, Bax, Bcl-2, p53, Fasl and TNF-α and neuronal survival (Fig. 5D and 5F), which suggests that a threshold JNK activity may be required in activating downstream genes and inducing neuronal cell death in this culture system [26]. Co-treatment with si-ERK did not change MAP2 + cell number and LDH release in $BRAF^{V600E}$-transduced cells (Fig. 5I). Despite reported role of ERK in neuronal survival [27] and a trend for reduced number of MAP2 + cells and increased LDH release at 120 h, there was no statistically significant difference between si-ERK and control-siRNA treated vector-transduced neurons at the time points investigated.

Enrichment of BRAF-related genes in pathways associated with Parkinson's disease

To explore associations of BRAF signaling with neurodegeneration, we performed GO and KEGG pathway enrichment analyses of the GDS2821 dataset, which consists of gene expression profiles in the SN from postmortem brains of patients with Parkinson's disease (n = 16). The BRAF-related genes were significantly enriched in chemical synaptic transmission, protein polyubiquitination, proteasome-mediated ubiquitin-dependent protein catabolic process, etc. at the BP levels; mitochondrial inner membrane, nucleus, cytoplasm, etc. at the CC levels and protein binding, ubiquitin-protein transferase activity, ligase activity, etc. at the MF levels (Fig. 6A and Table S1). KEGG pathway analysis indicated that metabolic pathways, oxidative phosphorylation, and synaptic vesicle cycle, were mostly associated with the BRAF-related genes (Fig. 6B and Table S2).

Discussion

Our study using multiple *in vitro* systems provides evidence that oncogenic $BRAF^{V600E}$ induces 1) proliferation and activation of microglial cells through activated ERK but not activated JNK; 2) neuronal cell death directly through activated JNK but not activated ERK, and indirectly through ERK-activated microglia; 3) proliferation of astrocytes. $BRAF^{WT}$ showed no effects or minor effects in the same direct as $BRAF^{V600E}$, suggesting either specificity of the mutant BRAF actions or more likely, the dose effects of BRAF activation.

Normal BRAF signaling and the Ras-Raf-MEK-ERK pathway control survival, proliferation, senescence, and differentiation of cells as results of their responses to environmental cues. $BRAF^{V600E}$ and the constitutive activation of the pathway induce proliferation and cancer transformation either alone or in synergy with other oncogenic insults in a wide range of dividing cell [28]. In melanocytes, for example, $BRAF^{V600E}$ induces MEK and ERK and promotes cell growth and tumorigenicity [29]. In addition to malignant melanomas, $BRAF^{V600E}$ is also common in primary brain tumors of glial origin including pleomorphic xanthoastrocytoma, ganglioglioma, epithelioid glioblastoma, and gliomas [30]. Our findings that $BRAF^{V600E}$ induced proliferation of astrocytes in primary cortical mixed culture and primary astrocytes are consistent with previously reported increased cell proliferation in primary mouse astrocytes overexpressing $BRAF^{V600E}$ by retrovirus transduction [31]. The overgrowing astrocytes appear to be active in producing cytokines and chemokines, neurotrophic GDNF, and activating anti-oxidant genes, at least at mRNA levels. Although whether physically proximal $BRAF^{V600E}$-expressing astrocytes may influence neurons such as in the case of the mixed culture is unknown, neither trophic nor toxic effects were observed in neurons treated with conditioned medium from astrocytes expressing $BRAF^{V600E}$. The lack of effects might be explained by the relatively small extent of ERK activation and differential changes in downstream effectors.

$BRAF^{V600E}$ similarly activated ERK in BV2 and primary microglial cells. Proliferation and activation of microglia following $BRAF^{V600E}$ expression were clearly demonstrated at both morphological and functional levels. Primary microglial cells expressing $BRAF^{V600E}$ exhibited classical activation state with induction of iNOS and NF-κB as well as various cytokines and chemokines such as TNF-α, IL-1 β, IL-6, superoxide, ROS and NO. Our demonstration of the critical role of ERK in mediating microglial proliferation and activation confirms ERK as the downstream effector of the $BRAF^{V600E}$ action [15, 32].

The proliferative and activating responses of microglial cells to $BRAF^{V600E}$ expression conveyed their impact on neuronal survival. Neurotoxicity of conditioned medium from microglial cells overexpressing $BRAF^{V600E}$ is likely a result of proinflammatory cytokines and chemokines secreted by the activated microglial cells. Studies from cancer especially melanoma field have demonstrated $BRAF^{V600E}$ and altered immunity in tumor initiation and progression [33]. Particularly microphages may play a critical role in melanoma resistance to BRAF inhibitors [34]. As the resident macrophage within CNS, microglia have long been associated with neurological pathologies. Mass et al. reported that a somatic $BRAF^{V600E}$ mutation in yolk-sac erythro-myeloid progenitors, which give rise to microglia during development,

resulted in clonal expansion of tissue-resident macrophages, including microglia with activated ERK [15]. The neurodegenerative disorder developed late in this mouse model, including synaptic loss and neuronal death were driven by ERK-activated microglia and were preventable by BRAF inhibition. The model closely resembles late-onset neurodegenerative disease observed in patients with histiocytoses, which are clonal myeloid diseases characterized by inflammatory lesions [35]. Activating somatic mutations in the RAS–MEK–ERK pathway, predominantly $BRAF^{V600E}$ are strongly associated with histiocytosis, and $BRAF^{V600E}$ status also predicts risk of neurodegenerative complications in these conditions. ERK activation in activated microglia has also been implicated in common age-related neurodegenerative disorders such as Parkinson's disease and Alzheimer's disease [36, 37]. Our study further demonstrated *in vitro* a clear causal link between $BRAF^{V600E}$-induced and ERK-mediated activated microglia and neuronal cell death that does not require physical proximity as *in vivo*.

The $BRAF^{V600E}$ expression in neurons likewise directly caused cell death. This direct effect of the mutant BRAF on neurons, however, was not mediated by ERK but JNK. The JNK/c-Jun pathway in $BRAF^{V600E}$ melanomas is involved in adaptive responses to targeted therapy [38, 39]. The pathway may be paradoxically upregulated following BRAF inhibitor treatment, which may promote cancer cells becoming quiescent and therefore resistant to drug-induced apoptosis. Both EKR and JNK are activated by $BRAF^{V600E}$ expression in both primary microglia and neurons in the present study. Although inhibition of endogenous ERK and JNK in vector treated cells did not appear to affect cell survival and proliferation in either neurons or glial cells in our systems, which may be explained by incomplete block of either using siRNA approach, both ERK and JNK are necessary for neuronal development and maintenance, and their abnormal activation can lead to dysfunction and cell death. JNK activation in neurons is generally considered proapoptotic in various conditions [26, 40]. A recent study reported that the JNK pathway was activated in neurotoxic amyloid peptide $A\beta_{42}$-treated neurons or neurons from a transgenic mouse model of Alzheimer's disease, which resulted in aberrant cell cycle re-entry and caused neuronal apoptosis [41]. ERK signaling, on the other hand, can be either protective or associated with promotion of neuronal cell death depending on the contexts [42]. Growing evidence supports that activation of ERK can mediate cell death in several neuronal systems [43, 44]. BRAF itself have been shown to play an essential role in neuron differentiation and axon growth [45]. BRAF activation was found to be neuroprotective through inhibition of activating transcription factor (ATF)-3 of the ATF/cAMP response element binding protein family [46]. The proliferative effect in microglia mediated by ERK and the toxic effect in neurons mediated by JNK following $BRAF^{V600E}$ expression in our systems further highlight specific cellular contexts in dictating effectors and thus consequences of BRAF activation.

Much effort has been made in developing BRAF inhibitors for targeted cancer therapy. Consistent overall with our results that BRAF activation is neurotoxic, dabrafenib, a BRAF inhibitor and melanoma drug was found to inhibit c-Jun and to activate ERK, paradoxically, and to be neuroprotective in SH-SY5Y cellular and mouse models of Parkinson's disease, though it is unknown whether the protection by dabrafenib was through direct inhibition of BRAF in neurons or indirect inhibition of activated microglia in the *in vivo* models[16]. The aforementioned mouse study showed that BRAF inhibitor PLX4720 was neuroprotective

through apparent inhibition of activated microglia [15]. Microglial activation contributes to neurodegeneration in Parkinson's disease [47]. Interestingly, Parkinson's disease and melanoma are positively linked epidemiologically [48]. Our GO and KEGG analyses of Parkinson's disease SN gene expression data indicated enrichment of the BRAF-related genes in KEGG pathways such as oxidative phosphorylation and synaptic vesicle cycle, which have been implicated in the pathophysiology of Parkinson's disease [49, 50]. Further exploring BRAF in Parkinson's disease-melanoma link in both *in vitro* and *in vivo* models may be important to better understand molecular mechanisms underlying this seemingly unusual link with potentials of repositioning BRAF targeting cancer drugs for the treatment of Parkinson's and other neurological diseases.

Conclusions

Our study identifies distinct outcomes mediated by distinct downstream effectors in dividing glial cells and in neurons *in vitro* following the same oncogenic BRAF mutational activation. While BRAF activation in dividing cells has been extensively studied, we are just beginning to understand possibly an important role of BRAF in neurons and neurological disorders as a result of either dysregulated BRAF in neurons or its impact on dividing cells such as microglia. Future studies should aim to further decipher interactions between neurons and glia in response to BRAF alterations at molecular levels and to explore the BRAF pathway targeting as a therapeutic strategy for neurological diseases.

Abbreviations

JNK: c-Jun amino-terminal kinase; BRAF: v-Raf murine sarcoma viral oncogene homolog B; MEK: mitogen activated protein kinase; ERK: extracellular signal-regulated kinase; CNS: central nervous system; RV: retrovirus; LV: lentivirus; MAP2: microtubule-associated protein 2; GFAP: glial fibrillary acidic protein; NF-κB: nuclear factor kappa-B; PVDF: polyvinylidene fluoride; IL-1β: Interleukin-1β; IL-6: Interleukin-6; TNF α: tumor necrosis factor α; SN: substantia nigra; NCBI: National Center for Biotechnology Information; GEO: Gene Expression Omnibus; GO: gene ontology; BP: biological process; CC: cellular component; MF: molecular function; KEGG: Kyoto Encyclopedia of Genes and Genomes; MAP: mitogen-activated protein; p-MEK1/2: phosphorylated mitogen activated protein kinase 1/2; p-ERK1/2: phosphorylated extracellular signal-regulated kinase 1/2; COX2: cyclooxygenase 2; Nrf2: nuclear factor erythroid 2-related factor 2; HO1: heme oxygenase 1; NQO1: quinone oxidoreductase 1; GCLC: glutamate cysteine ligase catalytic subunit; GCLM: glutamate cysteine ligase modifier subunit; GDNF: glial-derived neurotrophic factor; NF-κB: nuclear factor kappa-B; p-NF-κB p65: phosphorylated nuclear factor kappa-B p65; si-JNK: siRNA targeting c-Jun amino-terminal kinase; si-ERK: siRNA targeting extracellular signal-regulated kinase; iNOS: inducible NO synthase; LDH: lactate dehydrogenase; Bcl-2: B cell leukemia/lymphoma-2; Bax: B cell leukemia/lymphoma-2 associated X protein; FasL: Fas-ligand; ATF: activating transcription factor.

Declarations

Acknowledgements

Not applicable

Authors' contributions

Conceived and designed the study: QY and XC; Collected the data: QY; Contributed data or analysis tools: QY, NAK, and PW; Performed the analysis: QY and XC; Wrote the paper: QY and XC.

Funding

This work was supported by NIH (R01NS102735), the National Natural Science Foundation of China (82074355 and 81771379), and the Michael J. Fox Foundation for Parkinson's Research (MJFF) and the Aligning Science Across Parkinson's Initiative (ASAP) (ASAP-000312). Funders had no role in study design, data collection, analysis, or decision to publish the manuscript.

Availability of data and materials

The datasets used and/or analyzed during the current study are available from the corresponding author upon reasonable request.

Ethics approval and consent to participate

Not applicable.

Consent for publication

Not applicable.

Competing interests

The authors declare that there are no conflicts of interest.

Declaration of Interests

The authors declare no competing interests.

References

[1] Wellbrock, C., Karasarides, M., Marais, R. (2004). The RAF proteins take centre stage. Nat Rev Mol Cell Biol *5*, 875–885.

[2] Galabova-Kovacs, G., Catalanotti, F., Matzen, D., Reyes, G.X., Zezula, J., Herbst, R., Silva, A., Walter, I., Baccarini, M. (2008). Essential role of B-Raf in oligodendrocyte maturation and myelination during postnatal central nervous system development. J Cell Biol *180*, 947–955.

[3] Tien, A.C., Tsai, H.H., Molofsky, A.V., McMahon, M., Foo, L.C., Kaul, A., Dougherty, J.D., Heintz, N., Gutmann, D.H., Barres, B.A., Rowitch, D.H. (2012). Regulated temporal-spatial astrocyte precursor cell

proliferation involves BRAF signalling in mammalian spinal cord. Development *139*, 2477–2487.

[4] Schreck, K.C., Grossman, S.A., Pratilas, C.A. (2019). BRAF Mutations and the Utility of RAF and MEK Inhibitors in Primary Brain Tumors. Cancers (Basel) *11*, 1262.

[5] Zaman, A., Wu, W., Bivona, T.G. (2019). Targeting Oncogenic BRAF: Past, Present, and Future. Cancers (Basel) *11*, 1197.

[6] Zhong, J. (2016). RAS and downstream RAF-MEK and PI3K-AKT signaling in neuronal development, function and dysfunction. Biol Chem *397*, 215–222.

[7] Frebel, K., Wiese, S. (2006). Signalling molecules essential for neuronal survival and differentiation. Biochem Soc Trans *34*, 1287–1290.

[8] Wojnowski, L., Zimmer, A.M., Beck, T.W., Hahn, H., Bernal, R., Rapp, U.R., Zimmer, A. (1997). Endothelial apoptosis in Braf-deficient mice. Nat Genet *16*, 293–297.

[9] Chen, A.P., Ohno, M., Giese, K.P., Kuhn, R., Chen, R.L., Silva, A.J. (2006). Forebrain-specific knockout of B-raf kinase leads to deficits in hippocampal long-term potentiation, learning, and memory. J Neurosci Res *83*, 28–38.

[10] Lim, C.S., Kang, X., Mirabella, V., Zhang, H., Bu, Q., Araki, Y., Hoang, E.T., Wang, S., Shen, Y., Choi, S., et al. (2017). BRaf signaling principles unveiled by large-scale human mutation analysis with a rapid lentivirus-based gene replacement method. Genes Dev *31*, 537–552.

[11] Goz, R.U., Akgul, G., LoTurco, J.J. (2020). BRAFV600E expression in neural progenitors results in a hyperexcitable phenotype in neocortical pyramidal neurons. J Neurophysiol *123*, 2449–2464.

[12] Koh, H.Y., Kim, S.H., Jang, J., Kim, H., Han, S., Lim, J.S., Son, G., Choi, J., Park, B.O., Heo, W.D., et al. (2018). BRAF somatic mutation contributes to intrinsic epileptogenicity in pediatric brain tumors. Nat Med *24*,1662–1668.

[13] Urosevic, S., Collins, P., Muetzel, R., Lim, K., Luciana, M. (2012). Longitudinal changes in behavioral approach system sensitivity and brain structures involved in reward processing during adolescence. Dev Psychol *48*, 1488–1500.

[14] Mass, E., Jacome-Galarza, C.E., Blank, T., Lazarov, T., Durham, B.H., Ozkaya, N., Pastore, A., Schwabenland, M., Chung, Y.R., Rosenblum, M.K., et al. (2017). A somatic mutation in erythro-myeloid progenitors causes neurodegenerative disease. Nature *549*, 389–393.

[15] Uenaka, T., Satake, W., Cha, P.C., Hayakawa, H., Baba, K., Jiang, S.Y., Kobayashi, K.,Kanagawa, M., Okada, Y., Mochizuki, H., et al. (2018). In silico drug screening by using genome-wide association study data repurposed dabrafenib, an anti-melanoma drug, for Parkinson's disease. Human Molecular Genetics *27*, 3974–3985.

[16] Encinas, M., Iglesias, M., Liu, Y., Wang, H., Muhaisen, A., Ceña, V., Gallego, C., Comella. J.X. (2000). Sequential treatment of SH-SY5Y cells with retinoic acid and brain-derived neurotrophic factor gives rise to fully differentiated, neurotrophic factor-dependent, human neuron-like cells. J Neurochem 75, 991–1003.

[17] Hilgenberg, L.G., Smith, M.A. (2007). Preparation of dissociated mouse cortical neuron cultures. J Vis Exp *10*, 562.

[18] Sciarretta, C., Minichiello, L. (2010). The preparation of primary cortical neuron cultures and a practical application using immunofluorescent cytochemistry. Methods of Molecular Biology *633*, 221–231.

[19] Roy, J. (2018). Primary microglia isolation from mixed cell cultures of neonatal mouse brain tissue. Brain Research *1689*, 21–29.

[20] Lian H, Roy E, Zheng H. (2016). Protocol for Primary Microglial Culture Preparation. Bio Protoc 6, e1989.

[21] Ahlemeyer B, Baumgart-Vogt E. (2005). Optimized protocols for the simultaneous preparation of primary neuronal cultures of the neocortex, hippocampus and cerebellum from individual newborn (P0.5) C57Bl/6J mice. J Neurosci Methods *149*, 110–120.

[22] Kawakami H, Huang S, Pal K, Dutta SK, Mukhopadhyay D, Sinicrope FA. (2016). Mutant BRAF Upregulates MCL-1 to Confer Apoptosis Resistance that Is Reversed by MCL-1 Antagonism and Cobimetinib in Colorectal Cancer. Mol Cancer Ther *15*, 3015–3027.

[23] Ritchie, M.E., Phipson, B., Wu, D., Hu, Y., Law, C.W., Shi. W., Smyth, G.K. (2015). limma powers differential expression analyses for RNA-sequencing and microarray studies. Nucleic Acids Res *43*, e47.

[24] Huang da W, Sherman BT, Lempicki RA. (2009). Systematic and integrative analysis of large gene lists using DAVID bioinformatics resources. Nat Protoc *4*, 44–57.

[25] Wan, P.T., Garnett, M.J., Roe, S.M., Lee, S., Niculescu-Duvaz, D., Good, V.M., Jones, C.M., Marshall, C.J., Springer, C.J., Barford, D., et al. (2004). Mechanism of activation of the RAF-ERK signaling pathway by oncogenic mutations of B-RAF. Cell *116*, 855–867.

[26] Hollville, E., Romero, S.E., Deshmukh, M. (2019). Apoptotic cell death regulation in neurons. FEBS J *286*, 3276–3298.

[27] Hossain, M.S., Ifuku, M., Take, S., Kawamura, J., Miake, K., Katafuchi, T. (2013). Plasmalogens Rescue Neuronal Cell Death through an Activation of AKT and ERK Survival Signaling. PLOS ONE *8*, e83508.

[28] Robinson, J.P., VanBrocklin, M.W., Guilbeault, A.R., Signorelli, D.L., Brandner, S., Holmen, S.L. (2010). Activated BRAF induces gliomas in mice when combined with Ink4a/Arf loss or Akt activation. Oncogene

29, 335–344.

[29] Wellbrock, C., Ogilvie, L., Hedley, D., Karasarides, M., Martin, J., Niculescuduvaz, D., Springer, C.J., Marais, R. (2018). V599EB-RAF is an Oncogene in Melanocytes. Cancer Research *64*, 2338–2342.

[30] Maraka S, Janku F. (2018). BRAF alterations in primary brain tumors. Discov Med *26*, 51–60.

[31] Gronych, J., Korshunov, A., Bageritz, J., Milde, T., Jugold, M., Hambardzumyan, D., Remke, M., Hartmann, C., Witt, H., Jones, D.T., et al. (2011). An activated mutant BRAF kinase domain is sufficient to induce pilocytic astrocytoma in mice. J Clin Invest 121, 1344–1348.

[32] Schreiner B, Greter M. (2017). EMPhasis on Mutant Microglia: Dysregulation of Brain Sentinels Induces Neurodegeneration. Cell Stem Cell *21*, 566–568.

[33] Kuske, M., Westphal, D., Wehner, R., Schmitz, M., Beissert, S., Praetorius, C., Meier, F.

(2018). Immunomodulatory effects of BRAF and MEK inhibitors: Implications for Melanoma therapy. Pharmacol Res *136*, 151–159.

[34] Wang, T., Feldman, G.M., Herlyn, M., Kaufman, R.E. (2015). The macrophage: Switches from a passenger to a driver during anticancer therapy. Oncoimmunology *4*, e1052929.

[35] Ribeiro, M.J., Idbaih, A., Thomas, C., Remy, P., Martin-Duverneuil, N., Samson, Y., Donadieu, J., Hoang-Xuan, K. (2008). 18F-FDG PET in neurodegenerative Langerhans cell histiocytosis : results and potential interest for an early diagnosis of the disease. J Neurol *255*, 575–580.

[36] Chen, M.J., Ramesha, S., Weinstock, L.D., Gao, T., Ping, L., Xiao, H. (2019). Microglial ERK activation is a critical regulator of pro-inflammatory immune responses in Alzheimer's disease. bioRxiv, 98215.

[37] Sarkar, S., Lu, E., Raymick, J., Hanig, J.P., Gu, Q. (2019). ERK/MAP Kinase Activation is Evident in Activated Microglia of the Striatum and Substantia Nigra in an Acute and Chronically-Induced Mouse Model of Parkinson's Disease. Current Neurovascular Research *15*, 336–344.

[38] Fallahisichani, M., Moerke, N.J., Niepel, M., Zhang, T., Gray, N.S., Sorger, P.K. (2015). Systematic analysis of BRAFV600E melanomas reveals a role for JNK/c-Jun pathway in adaptive resistance to drug-induced apoptosis. Molecular Systems Biology *11*, 797.

[39] Vin, H., Ojeda, S.S., Ching, G., Leung, M.L., Chitsazzadeh, V., Dwyer, D.W., Adelmann, C.H., Restrepo, M., Richards, K.N., Stewart, L.R., et al. (2013). BRAF inhibitors suppress apoptosis through off-target inhibition of JNK signaling. Elife *2*, e00969.

[40] Dhanasekaran, D.N., Reddy, E.P. (2017). JNK-signaling: A multiplexing hub in programmed cell death. Genes Cancer *8*, 682–694.

[41] Chauhan, M., Modi, P.K., Sharma, P. (2020). Aberrant activation of neuronal cell cycle caused by dysregulation of ubiquitin ligase Itch results in neurodegeneration. Cell Death Dis *11*, 441.

[42] Hutton, S.R., Otis. J.M., Kim, E.M., Lamsal, Y., Stuber, G.D., Snider, W.D. (2017). ERK/MAPK Signaling Is Required for Pathway-Specific Striatal Motor Functions. J Neurosci *37*, 8102–8015.

[43] Zhu, X,, Lee, H.G., Raina, A.K., Perry, G., Smith, M.A. (2002). The role of mitogen-activated protein kinase pathways in Alzheimer's disease. Neurosignals *11*, 270–281.

[44] Sun, J., Nan, G. (2017). The extracellular signal-regulated kinase 1/2 pathway in neurological diseases: A potential therapeutic target (Review). Int J Mol Med *39*, 1338–1346.

[45] Zhong, J., Li, X., McNamee, C., Chen, A.P., Baccarini, M., Snider, W.D. (2007). Raf kinase signaling functions in sensory neuron differentiation and axon growth in vivo. Nat Neurosci *10*, 598–607.

[46] Chen, H.M., Wang, L., D'Mello, S.R. (2008). Inhibition of ATF-3 expression by B-Raf mediates the neuroprotective action of GW5074. J Neurochem *105*, 1300–1312.

[47] Heneka, M.T. (2019). Microglia take centre stage in neurodegenerative disease. Nat Rev Immunol *19*, 79–80.

[48] Ye, Q., Wen, Y., Al-Kuwari, N., Chen, X.Q. (2020). Association Between Parkinson's Disease and Melanoma: Putting the Pieces Together. Front Aging Neurosci *12*, 60.

[49] Iglesias, E., Pesini, A., Garrido-Pérez, N., Meade, P., Bayona-Bafaluy, M.P., Montoya. J., Ruiz-Pesini, E. (2018). Prenatal exposure to oxidative phosphorylation xenobiotics and late-onset Parkinson disease. Ageing Res Rev 45, 24–32.

[50] Nemani, V.M., Lu. W., Berge, V., Nakamura, K., Onoa, B., Lee, M.K., Chaudhry, F.A., Nicoll, R.A., Edwards, R.H. (2010). Increased expression of alpha-synuclein reduces neurotransmitter release by inhibiting synaptic vesicle reclustering after endocytosis. *Neuron* 65, 66–79.

Tables

Table 1. The sequences of primers.

Gene	Forward	Reverse
Nrf2	ACTCCCTGCAGCAAACAAGAG	TTTTTCTTAACATCTGGTTCTTACTTTT
HO-1	GCCCTGCCCTTCAGCAT	AGCTGCCACATTAGGGTGTCTT
GCLC	GATGCTGTCTTGCAGGGAATG	AGCGAGCTCCGTGCTGTT
GCLM	ACAGGTAAAACCAAATAGTAACCAAGTTAA	TGTTTAGCAAATGCAGTCAAATCTG
GDNF	TCTTTCGATATTGCAGCGGTT	GCTACGACGTGGGCTACAG
NQO1	TGGCCGAACACAAGAAGCTG	GCTACGAGCACTCTCTCAAACC
TNF-α	CCCTCACACTCAGATCATCTTCT	GCTACGACGTGGGCTACAG
IL-1α	GACAGGGAACTTAGGGAGCA	TTGGCCATCTTGATTTCAGAGT
IL-1β	TTCAGGCAGGCAGTATCACTC	GAAGGTCCACGGGAAAGACAC
IL-6	TAGTCCTTCCTACCCCAATTTCC	TTGGTCCTTAGCCACTCCTTC
IL-10	GCTGGACAACATACTGCTAACC	ATTTCCGATAAGGCTTGGCAA
iNOS	CCCTTCCGAAGTTTCTGGCAGCAGC	GGCTGTCAGAGAGCCTCGTGGCTTTGG
COX2	GGAGAGACTATCAAGATAGTGATC	ATGGTCAGTAGACTTTTACAGCTC
c-Jun	ACTCGGACCTTCTCACGTC	GGTCGGTGTAGTGGTGATGT
Bax	AGACAGGGGCCTTTTTGCTAC	AATTCGCCGGAGACACTCG
Bcl-2	GCTACCGTCGTGACTTCGC	CCCCACCGAACTCAAAGAAGG
p53	CCCCTGTCATCTTTTGTCCCT	AGCTGGCAGAATAGCTTATTGAG
Fasl	CAGCCCATGAATTACCCATGT	ATTTGTGTTGTGGTCCTTCTTCT

Figures

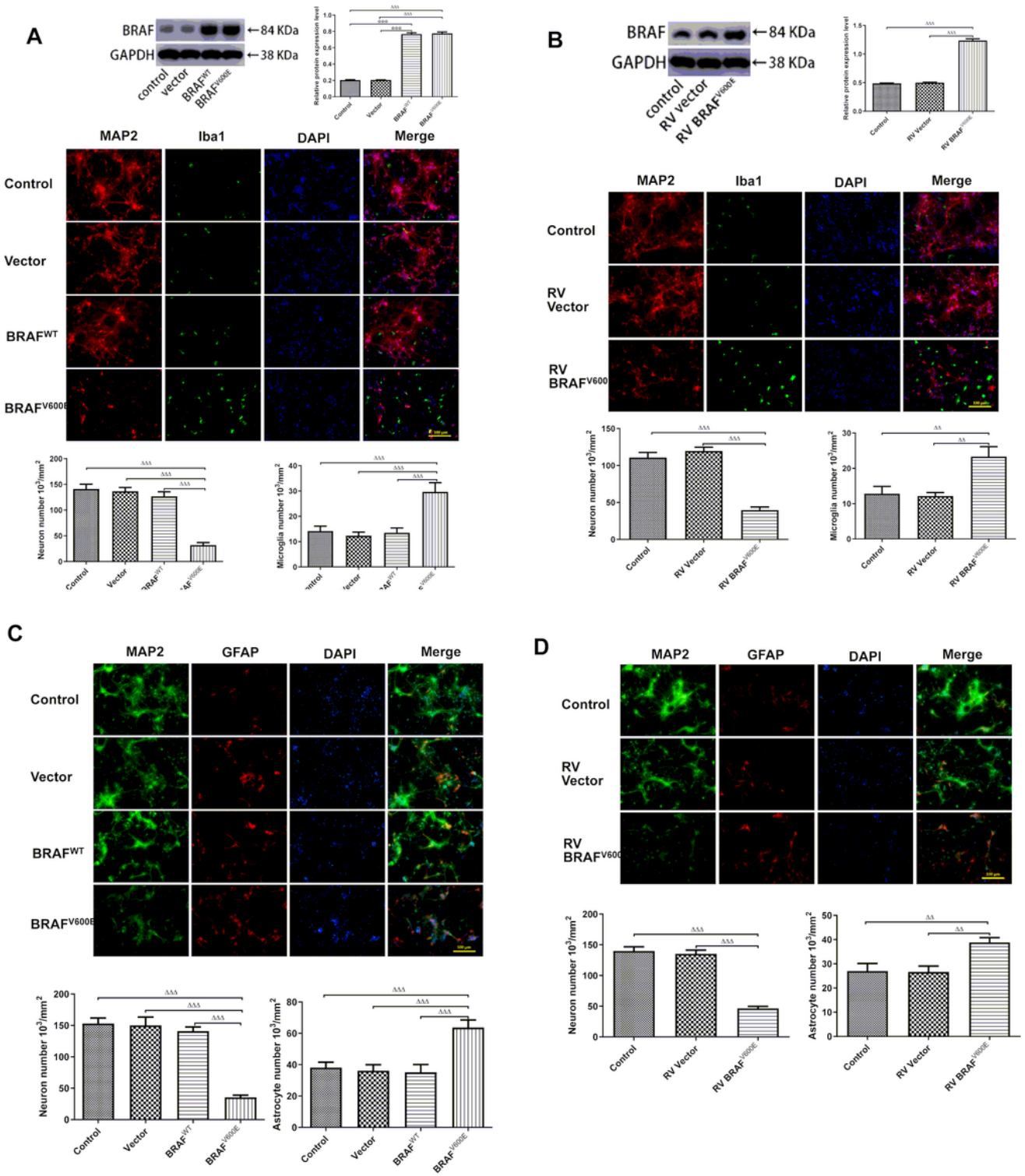

Figure 1

BRAFV600E expression leads to neuronal cell death and glial cell proliferation in primary mouse cortical mixed culture. Primary cortex mix cultures were prepared from C57BL/6J embryos. Cells were cultured in Neurobasal Media (NB-A) for 5 days, then transduced with viral vector, or BRAFWT, or BRAFV600E for 24 h and then cultured in NB-A medium for 96 h. (A) BRAF immunoblot and quantified BRAF expression level normalized to GAPDH, immunostaining for MAP2 and Iba1, and MAP2+ and Iba1+ cell counting in

cultures transduced with lentiviral BRAF vectors. (B) BRAF immunoblot and quantified BRAF expression level normalized to GAPDH, immunostaining for MAP2 and Iba1, and MAP2+ and Iba1+ cell counting in cultures transduced with retroviral (RV) BRAF vectors. (C) Immunostaining for MAP2 and GFAP, and MAP2+ and GFAP+ cell counting in cultures transduced with lentiviral BRAF vectors. (D) Immunostaining for MAP2 and GFAP, and MAP2+ cells and GFAP+ cell counting in cultures transduced with RV BRAF vectors. The nuclei were counterstained by DAPI, Bars = 100μm. ☆☆☆P < 0.001; ΔΔ P <0.01, ΔΔΔP < 0.001.

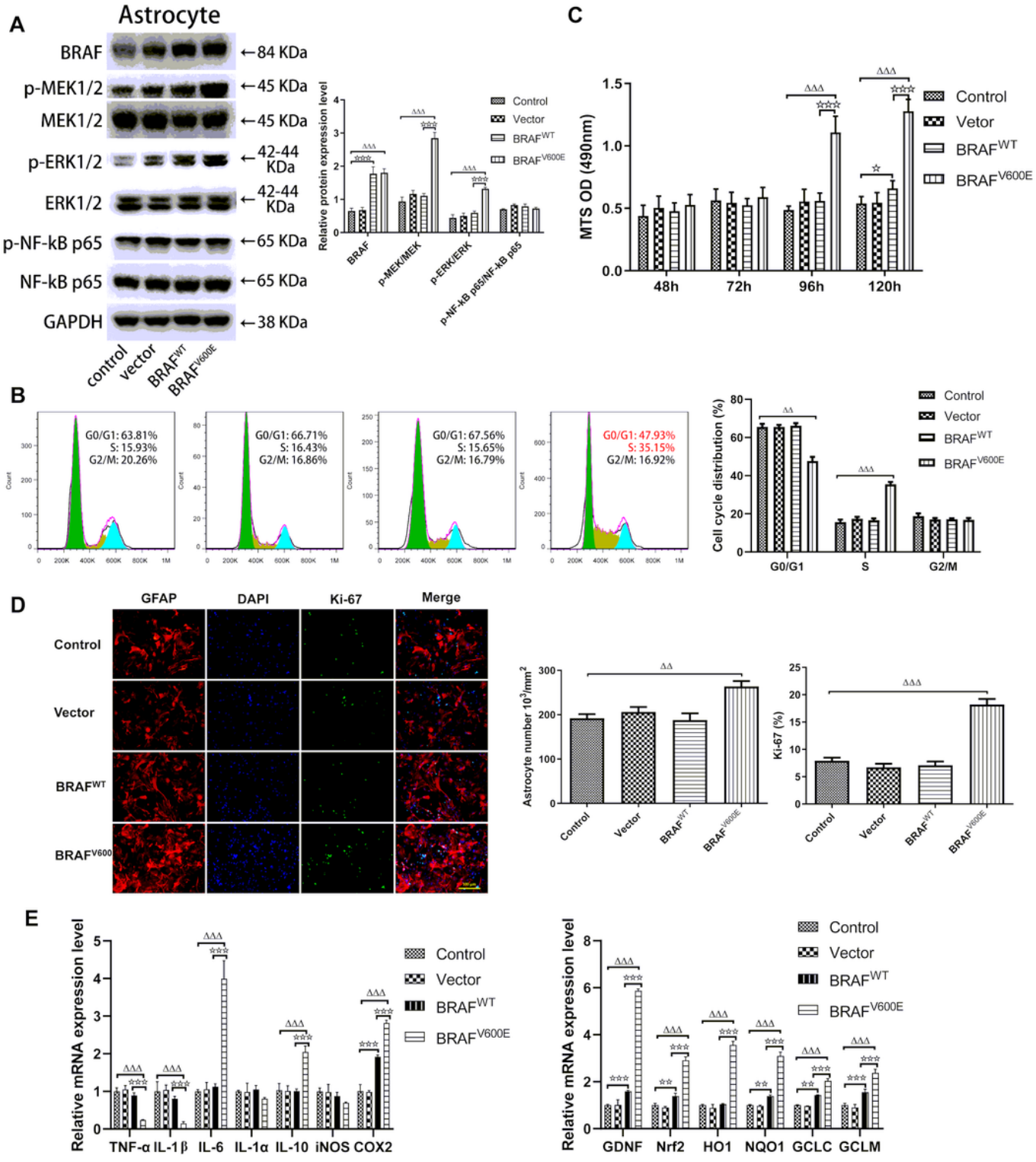

Figure 2

BRAFV600E expression in astrocytes promotes proliferation. Primary astrocytes were prepared from C57BL/6J embryos. Cells were transduced with lentiviral vector, or BRAFWT, or BRAFV600E for 24 h and then cultured in DMEM/F-12 medium for 96 h. (A) Immunoblotting for BRAF and related signaling proteins and quantified expression levels normalized to GAPDH. (B) Flow cytometry analysis of cell cycle. (C) Immunostaining for GFAP and Ki-67, GFAP+ cell counting, and % of Ki-67+ astrocytes (Bar = 100μm). (D) MTS cell viability assay at 48 h, 72 h, 96 h and 120 h following viral transduction. (E) qPCR analysis of inflammatory and antioxidant markers normalized to GAPDH. ▯▯P < 0.01, ▯▯▯P < 0.001; ΔΔP < 0.01, ΔΔΔP < 0.001.

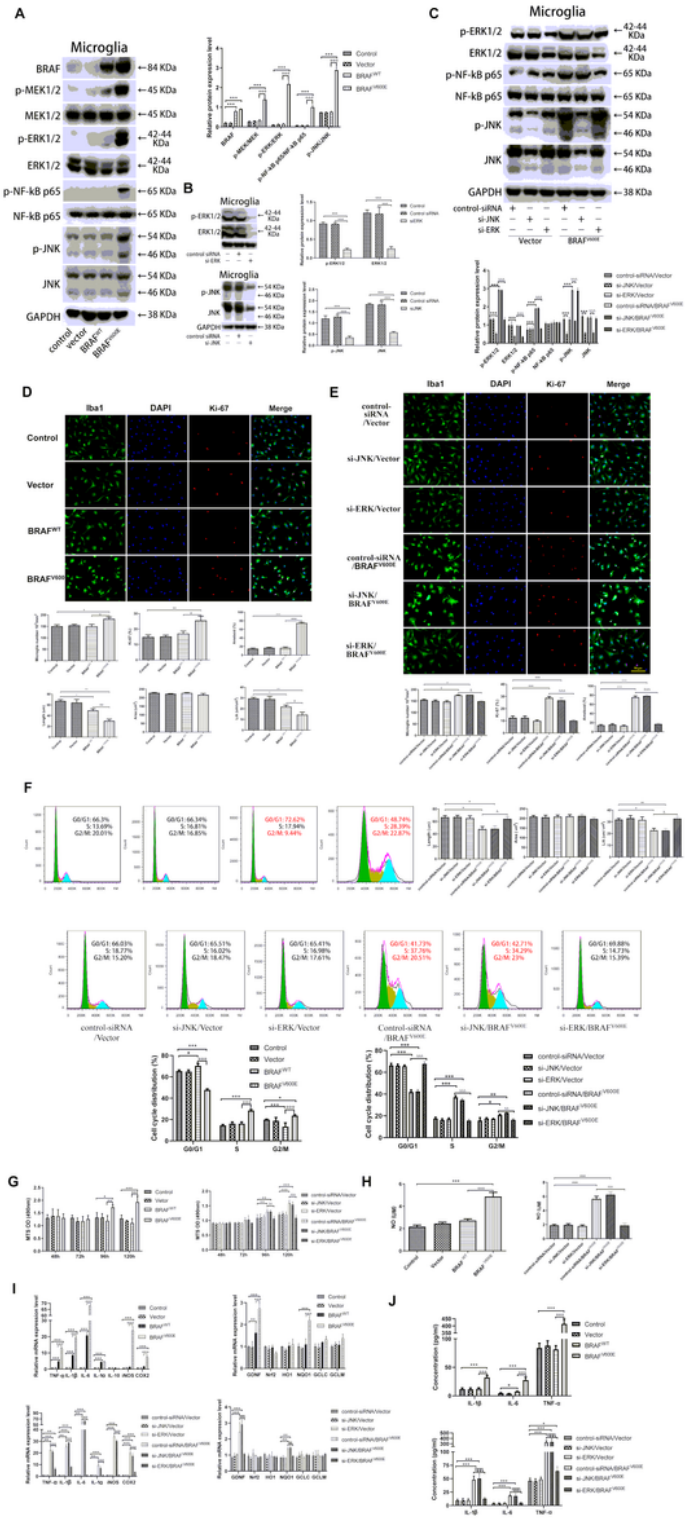

Figure 3

BRAFV600E expression in microglia induces cell proliferation and activation through ERK. Primary microglia cells were prepared from C57BL/6J embryos. Cells were transduced with lentiviral vector, BRAFWT and BRAFV600E for 24 h and then cultured in DMEM/F12 for 96 h. (A) Immunoblotting for BRAF and related signaling proteins and quantified expression levels normalized to GAPDH. (B) Cells were transfected with control-siRNA, or si-JNK, or si-ERK for 24 h before transduction with BRAF viral

vectors. Immunoblotting for BRAF, ERK, and JNK 48 h following viral transduction and quantified expression levels normalized to GAPDH. (C) Cells were transfected with control-siRNA, or si-JNK, or si-ERK for 24 h before transduction with BRAF viral vectors. Immunoblotting for BRAF and related signaling proteins and quantified expression levels normalized to GAPDH. Immunostaining for Iba1 and Ki-67, Iba1+ cell counting, and % of Ki-67+ microglia (Bar = 100μm), and quantitative morphological analyses (% of ameboid-like microglia cells, length, area, length to area ratio in cells without (D) and with siRNA transfection (E) (Bar = 50μm). (F) Flow cytometry analysis of cell cycle. (G) MTS cell viability assay at 48 h, 72 h, 96 h and 120 h following viral transduction. (H) NO release in culture media by Griess reaction. (I) qPCR analysis of inflammatory and antioxidant markers in cells normalized to GAPDH. (J) IL-1β, IL-6, TNF-α levels in culture medium measured by ELISA. Data are represented as mean ± SEM, n=9. *P < 0.05, **P < 0.01, ***P < 0.001; P < 0.05, P < 0.001; ΔΔΔP < 0.001.

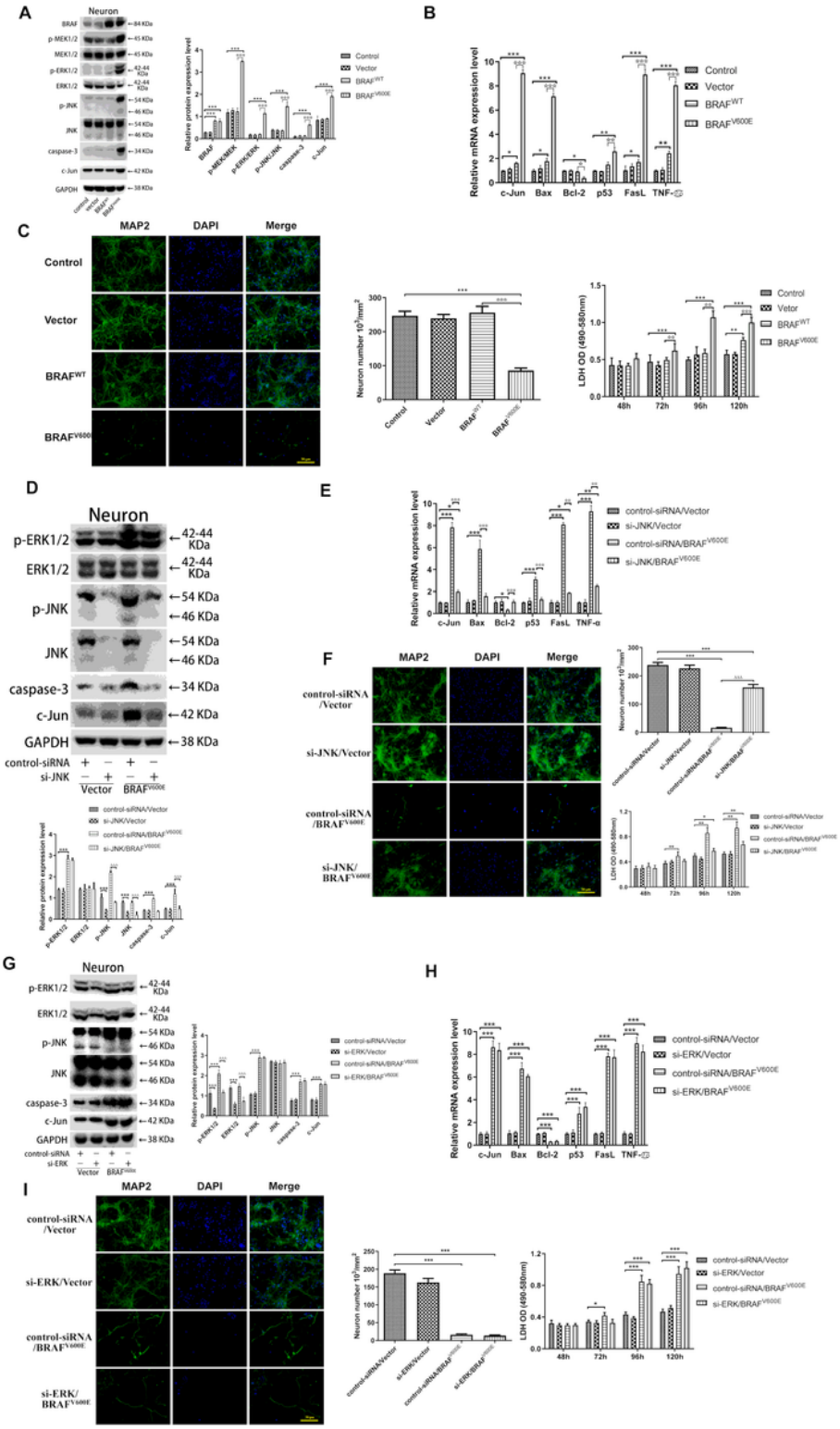

Figure 4

Conditioned medium from BRAFV600E-expressing microglial cells but not astrocytes induces neuronal cell death. Primary cortex neurons were prepared from C57BL/6J embryos and cultured for 5 days, the original medium was then replaced with conditional medium for 72 h. (A) Immunostaining for MAP2 (Bar = 50 μm) and MAP2+ cell counting, LDH release in neurons treated with conditioned medium from primary astrocytes transduced with lentiviral BRAF vectors. (B) Immunostaining for MAP2 (Bar = 50 μm)

and MAP2+ cell counting in neurons treated with conditioned medium from primary microglia transduced with lentiviral BRAF vectors with and without siRNA transfection. (C) LDH release from neurons treated with conditioned medium from primary microglia transduced with lentiviral BRAF vectors with and without siRNA transfection. *P < 0.05, **P < 0.01, ***P < 0.001; ▯P < 0.05, ▯▯P < 0.01, ▯▯▯P < 0.001; ΔΔΔP < 0.001.

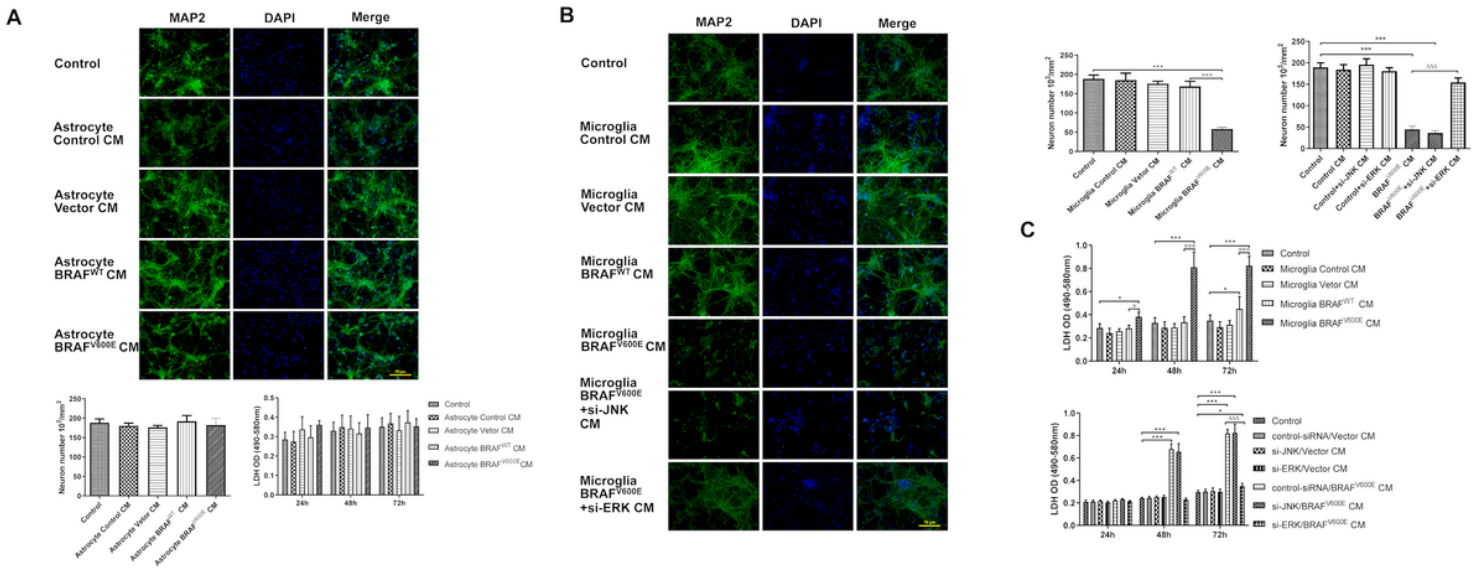

Figure 5

BRAFV600E expression in neurons promotes cell death through the JNK pathway. Primary cortex neurons were prepared from C57BL/6J embryos. Cells were cultured for 5 days, transduced with lentiviral vector, BRAFWT and BRAFV600E for 24 h, and then cultured in NB-A for 96 h. (A) Immunoblotting for BRAF and related signaling proteins and quantified expression levels normalized to GAPDH. (B) qPCR analysis c-Jun, Bax, Bcl-2, p53, Fasl and TNF-α normalized to GAPDH. (C) Immunostaining for MAP2 (Bar = 50 μm), MAP2+ cell counting, and LDH release. Primary cortex neurons were transfected with control-siRNA or si-JNK for 24 h before transduction with BRAF viral vectors. (D) Immunoblotting for BRAF and related signaling proteins and quantified expression levels normalized to GAPDH. (E) qPCR analysis of c-Jun, Bax, Bcl-2, p53, Fasl and TNF-α normalized to GAPDH. (F) Immunostaining for MAP2 (Bar = 50 μm), MAP2+ cell counting, and LDH release. Primary cortex neurons were transfected with control-siRNA or si-ERK for 24 h before transduction with BRAF viral vectors. (G) Immunoblotting for BRAF and related signaling proteins and quantified expression levels normalized to GAPDH. (H) qPCR analysis of c-Jun, Bax, Bcl-2, p53, Fasl and TNF-α normalized to GAPDH. (I) Immunostaining for MAP2 (Bar = 50 μm), MAP2+ cell counting, and LDH release. *P < 0.05, ***P < 0.001; ▯P < 0.05, ▯▯▯P < 0.001; ΔΔΔP < 0.001.

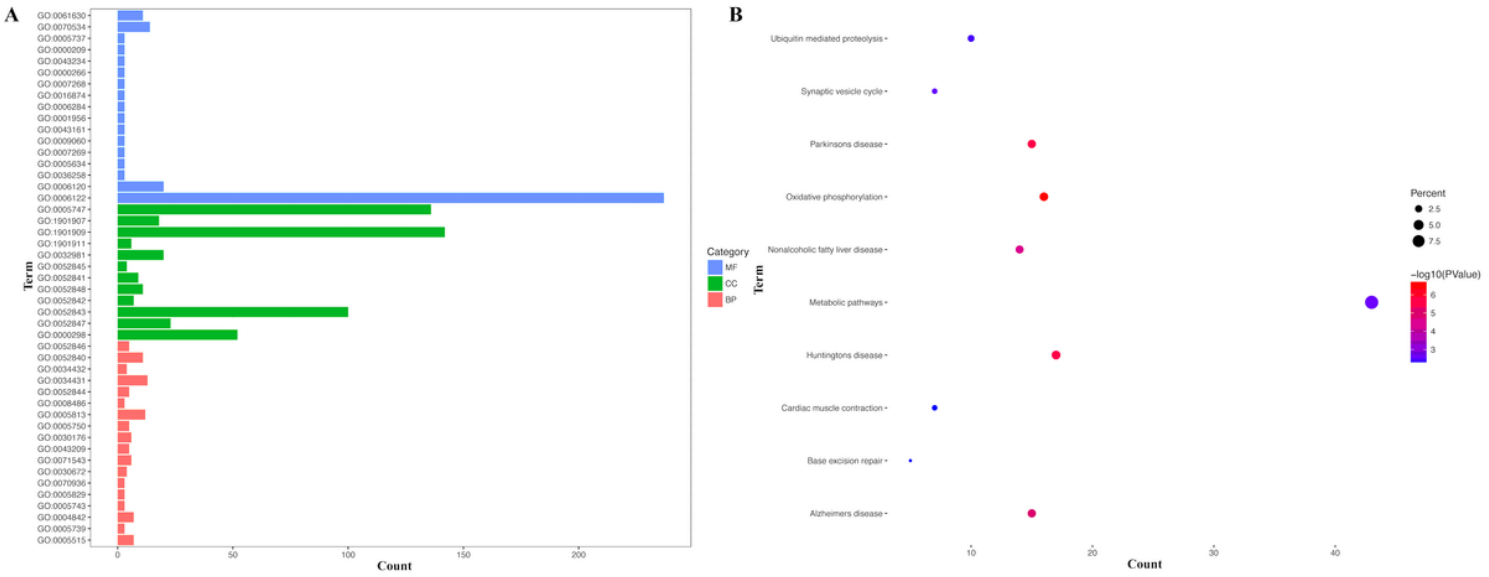

Figure 6

Enrichment of BRAF-related genes in the substantia nigra from patients with Parkinson's disease. Gene expression data from postmortem brains of patients with Parkinson's disease was collected from the GDS2821 cohort (n=16). (A) Gene ontology (GO) analysis at the molecular function (MF), the cellular component (CC), and the biological process (BP)levels. (B) Kyoto Encyclopedia of Genes and Genomes (KEGG) analysis.

Supplementary Files

This is a list of supplementary files associated with this preprint. Click to download.

- FigS1.tif
- FigS2.tif
- FigS3.tif